Activated carbon–carbon nanotube composite porous film for supercapacitor applications

Pierre-Louis Taberna [a], Geoffroy Chevallier [a], Patrice Simon [a,*],
Dominique Plée [b], Thierry Aubert [b]

[a] *CIRIMAT, UMR CNRS 5085, 118 Route de Narbonne, 31062 Toulouse Cedex 4, France*
[b] *ATOFINA, Groupe de Recherche de Lacq, BP 354, 64170 LACQ, France*

Abstract

Activated carbon/carbon nanotube composite electrodes have been assembled and tested in organic electrolyte (NEt_4BF_4 1.5 M in acetonitrile). The performances of such cells have been compared with pure activated carbon-based electrodes. CNTs content of 15 wt.% seems to be a good compromise between power and energy, with a cell series resistance of 0.6 Ω cm^2 and an active material capacitance as high as 88 F g^{-1}.

1. Introduction

Supercapacitors are electrochemical energy storage devices able to purchase high specific power. This particular characteristic, associated with an energy density higher than classic dielectric capacitors, makes them already useful in power electronics applications in small size devices. With the performances improvement and the cost reduction induced by important R&D efforts during the last 5 years, large supercapacitors cells are now thought to be used in automotive transportation, for instance integrated into hybrid electric vehicle (HEV). In the latter, supercapacitors could be used for engine starting (stop and go function), acceleration (boost function) and regenerative braking (energy recovery function).

Three different types of supercapacitors are commonly described in literature [1], depending on the nature of the active material used: conducting polymer [2,3], metal-oxide [4] and activated carbon [5–7].

In these systems, activated carbon-based supercapacitors using organic electrolyte are generally thought to be the most promising system, presenting the best performances/cost compromise [8]. The active material used in supercapacitors is a high surface area carbon, activated via a chemical or/and a physical route [9,10]. Energy is stored under electrostatic form, by reversible adsorption of the ions of the electrolyte. Specific capacitance of the activated carbon in organic electrolytes is around 100–130 F g^{-1}. The absence of charge-transfer redox reactions, such as in conventional batteries, led to the increase of the power density. Typical values for energy and power densities for commercial devices using organic electrolytes are, respectively, around 5 Wh/kg and 5 kW/kg.

* Corresponding author. Fax: +33 5 61 55 61 63.
 E-mail address: simon@chimie.ups-tlse.fr (P. Simon).

Carbon nanotubes (CNTs) have been extensively studied in supercapacitor applications [11–15]. Numerous papers have been focused on the use of CNTs as active material, due to their exceptional properties: a high electronic conductivity, an unique pore structure and a high usage efficiency of their specific surface area. The most important part of the work was focused on aqueous devices (sulphuric acid or KOH electrolytes), where CNTs specific capacitance reaches values as high as $180 \, \text{F} \, \text{g}^{-1}$ [16]. But the low electrochemical stability potential window in aqueous media (i.e. 1.2 V theoretically) limits the energy density stored in such devices.

The use of NTCs in non-aqueous electrolytes is less described in the literature. One of the reason is the difficulty to prepare, assemble and test supercapacitor cells in H_2O and O_2 free atmosphere. But the main reason is the low specific capacitance exhibited by CNTs in organic electrolytes (around $40 \, \text{F} \, \text{g}^{-1}$) as compared to activated carbon (100–$130 \, \text{F} \, \text{g}^{-1}$). Additionally, the cost of the CNTs prohibits today their utilization in systems where low-cost is needed.

In this paper, we discuss results obtained when using CNTs–activated carbon mixtures as active material in composite electrodes for supercapacitors in non-aqueous electrolyte. Electrochemical behavior, specific capacitance, specific resistance and cycling performances will be discussed.

2. Experimental

Current collectors are constituted by expanded aluminum 1050 current collectors laminated to 150 μm thick. The collectors are mechanically polished with 180-grade glass paper. A conducting paint is applied on the aluminum current collectors using the spray technique in order to improve the contact at the collector/active material interface. The conducting paint is polyurethane-based containing 76% tri-isocyanate hardener and 24% polyalcohol base, charged with 30 wt.% of acetylene black. Current collectors are dried several hours under vacuum after painting.

2.1. Active material tested

The precursor of the porous activated carbon (AC) is coconut shell supplied by the CECA Company. The activation was made by thermal treatment and the specific surface is 1440 m^2/g. This activated carbon is a microporous carbon.

The carbon nanotubes (NTCs) were synthesized by the ATOFINA Company by the chemical vapor deposition process: ethylene decomposition at 650–700 °C on Fe-based catalyst deposited on alumina. This process lead to multiwall carbon nanotubes (MWCNTs) with an average external diameter between 10 and 30 nm. A chemical treatment in sulfuric acid solution is performed in order to decrease the Al_2O_3 and Fe content. In the same time, the ash content is decreased down to 2.5 wt.%. The chemical composition is as follows: 0.02% SiO_2, 0.3% Al_2O_3 and 1.9% Fe_2O_3.

Active material is a mixture of the activated carbon and CNTs with 5% of poly-tetrafluoroethylene. After drying, active material is laminated onto 4 cm^2 treated aluminum current collectors. The experimental process has been described elsewhere [6].

2.2. 4 cm^2 Supercapacitors cells

Two-electrode 4 cm^2 supercapacitors cells were built by assembling two 4 cm^2 electrodes between 2 mm thick PTFE plates, inside a Mbräun glove box (H_2O and O_2 content lower than 1 ppm). A porous non-woven polymeric film was used as the separator. The system was kept under pressure with stainless steel clamps (16 kg/cm^2). Two-electrode cells were set in sealed Altuglass box to ensure air tightness, for the cells to be tested outside the glove box. This assembly ensures a relative tightness about 10 days, the water content becoming then too high to keep constant the characteristics of the cells.

The electrolyte used is a solution of NEt_4BF_4 1.5 M (recrystallized in methanol) in acetonitrile (containing less 10 ppm of water).

Galvanostatic cycling tests were carried out with an Arbin BTS2000 battery tester between 0 and 2.3 V. All the experiments were carried out at room temperature.

3. Results and discussion

Two-electrode supercapacitor cells were assembled with various active material composition, by mixing appropriate amounts of activated carbon and carbon nanotubes. The PTFE content in the active material was kept

constant at 5 wt.%. The active material mass was kept constant in all the experiment at 60 mg per electrode, i.e. 15 mg/cm^2. The different cells were cycled at ± 5 mA/cm^2 between 0 and 2.3 V in the organic electrolyte: NEt$_4$BF$_4$ 1.5 M in ACN.

Fig. 1 presents a typical potential–time plot obtained during galvanostatic charge/discharge for the cells.

The shape of the curve is linear in the potential range studied, proving the absence of Faradaic reactions. The capacitance of the cell was calculated from the slope of the $E = f(t)$ curves, using Eq. (1):

$$C = \frac{I}{\left(\frac{dV}{dt}\right)} \tag{1}$$

where C is the capacitance of the cell in farad, I the discharge current in ampere (A) and dV/dt is the slope in volt per second (V s^{-1}).

In a symmetrical system, the specific capacitance $C_{m_{AM}}$ in farad per gram of activate material (F g^{-1}) is related to the capacitance of the cell C by (2):

$$C_{m_{AC}} = \frac{2C}{m_{AM}} \tag{2}$$

where m_{AM} is the weight (g) per electrode of activate material, i.e. CNTs and activated carbon.

The equivalent series resistance (ESR) is measured during a 1 ms current pulse; the related potential is recorded and the ratio gives the ESR. This ESR corresponds to the one measured at 1 kHz on the electrochemical impedance spectroscopy plots, where the imaginary part $Z'' = 0$. It corresponds to the 1 kHz resistance.

Fig. 2 presents the specific resistance change of the two-electrode cells versus the NTCs weight content in the active material, measured at the 100th cycle.

The specific resistance of the cell using only activated carbon is 0.8 Ω cm^2. This is a good result in a non-aqueous electrolyte, showing power capability of these electrodes. This low resistance value is linked to the conducting properties of the active material film and also to the good contact between the active material and the painted Al current collectors.

The dispersion of the CNTs in the active material is made as follows. Desired amounts of activated carbon and CNTs powders are mixed together and then added in ethanol to obtain a suspension (100 ml ethanol/3 g powder).
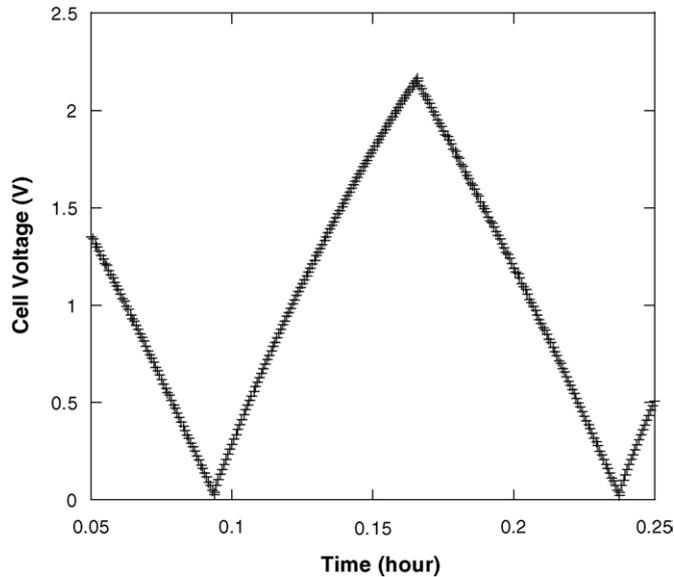
Fig. 1. Example of a charge/discharge plot at constant current (10 mA/cm^2) obtained for the different supercapacitor cells; active material weight: 60 mg per electrode; electrolyte NEt$_4$BF$_4$ 1.5 M in acetonitrile.
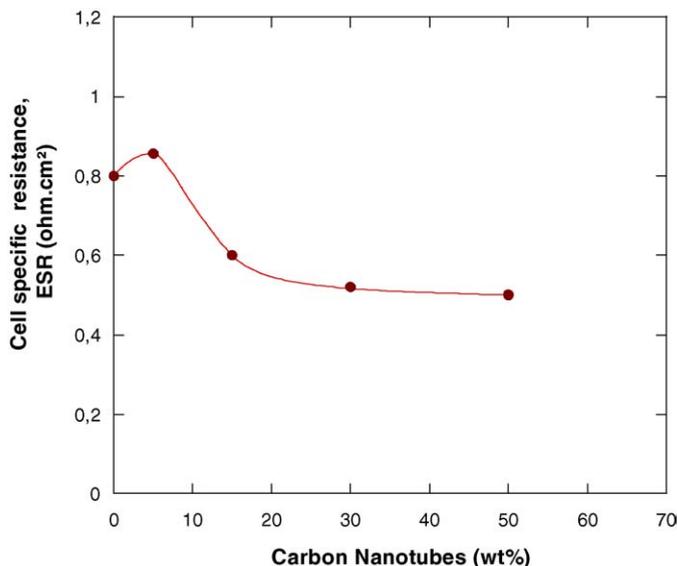
Fig. 2. ESR change of the cells vs. the active material MWCNTs content, up to 50 wt.%; active material weight: 60 mg per electrode; electrolyte NEt$_4$BF$_4$ 1.5 M in acetonitrile.

This suspension is ultrasonically treated, and then appropriate quantity of PTFE (60 wt.% suspension of PTFE in water) corresponding to 5 wt.% of dried activated carbon and CNTs is added.

From Fig. 2, it can be seen that the specific resistance of the cell is decreased from 0.8 down to 0.5 Ω cm^2 when the CNTs content increases up to 50 wt.%. It means an improvement of more than 30% of the power of the cell. For content lower than 5 wt.%, no effect can be seen on the specific resistance. The higher resistance measured is thought to come from an inhomogeneous dispersion of the CNTs inside the active material, and then is not significant. The decrease of the resistance is effective for NCTs content higher than 5 wt.%. The ESR decreases sharply down to 15 wt.% at 0.6 Ω cm^2 and tends to stabilize at 0.5 Ω cm^2.

The addition of CNTs amounts into the active material decreases the electronic resistance of the electrode by increasing the electronic percolation, as it is well known for instance in the insulating polymer/CNTs composites [17]. In this case, the electronic conductivity increases from a percolation threshold, around 1 wt.% of CNTs. Here, the decrease of the cell ESR occurs after 15 wt.%, that seems to be too high to be explained by an electronic percolation induced by the CNTs. Such behavior can be explained by taking into account the electronic and the ionic contributions to the ESR. The most important intrinsic contribution to the ESR in supercapacitor porous electrodes is the ionic resistance of the electrolyte in the separator and in the pores of the electrode. The ESR change versus CNTs content plot in Fig. 2 traduces the global effect of CNTs on both the electronic and ionic resistance. With increasing CNTs content, the electronic resistance is obviously decreased but above all the ionic part of the ESR is also decreased. CNTs are thought to modify the porous structure of the electrode and to allow faster ionic transfer kinetics inside the porous structure.

Fig. 3 presents the specific capacitance of the active material in F per total mass (CNTs and AC), measured at the 100th cycle. The activated carbon capacitance (without CNTs) is 92 F g^{-1}. This value is lower than the one obtained for low density highly activated carbon [18], but it is comparable to other coconut shell-based activated carbon [1].

When CNTs are added to the activated carbon, the specific capacitance decreases. It is an expectable result that is linked to the lower capacitance of the CNTs as compared to the activated carbon. Specific capacitance measured for a pure CNTs electrode is around 25 F g^{-1}. This low value prohibits the use of pure CNTs composite electrode for supercapacitor applications. The specific capacitance does not greatly change for low CNTs content (0–15 wt.%), from 92 down to 88 F g^{-1}. For higher content, it falls down to 50 F g^{-1} at 50 wt.% CNTs.

From the above results, taking into account the specific resistance and the specific capacitance of the active material, an optimum can be then found at 15 wt.% of CNTs in the active material. With such an electrode composition, the performance of a 4 cm^2 supercapacitor cell is as follows: 0.6 Ω cm^2 with a specific capacitance of 88 F g^{-1} of active material. This low content also allows to reduce the additional cost linked to the use of CNTs.
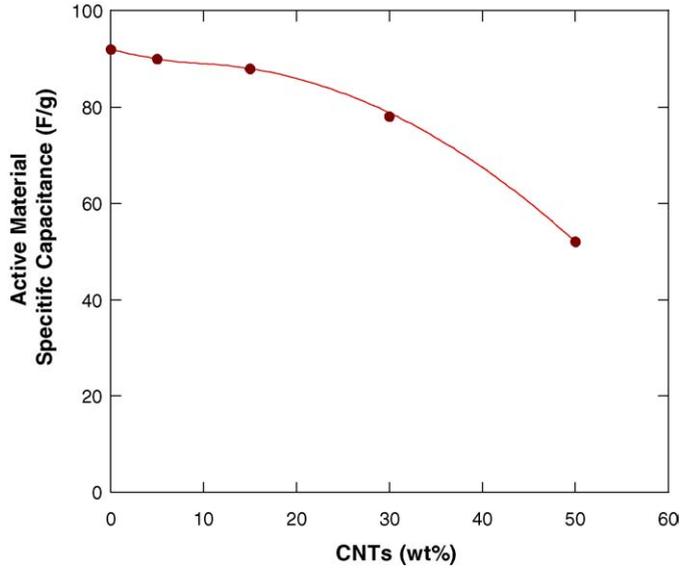
Fig. 3. Active material specific capacitance change vs. the MWCNTs content during galvanostatic cycling between 0 and 2.3 V; active material weight: 60 mg per electrode; electrolyte: NEt_4BF_4 1.5 M in acetonitrile.

Table 1 presents the volumetric capacitance obtained for pure activated carbon and CNTs/activated carbon electrodes in F/cm^3.

These values have been calculated using Eq. (3):

$$C_v = \frac{2C_{cell}}{Se}$$ (3)

where C_v is the volumetric capacitance, C_{cell} the cell capacitance, S the geometric surface of one electrode (4 cm^2 here) and e is the thickness of one active material paste. C_v is directly related to the volumetric energy stored in the system. For highly activated carbon, this value is generally found around 30 F/cm^3 due to the lower density of such carbons. For microporous carbons, such as coconut shell-based activated carbon, it can increase up to 40 F/cm^3 [11]. Here we obtain volumetric higher capacitance, meaning that the active material formulation fits with supercapacitor applications. This volumetric capacitance is in the same range as compared the one obtained (at higher costs) with mesoporous carbon synthesized by carbonization resins, around 50 F/cm^3 [19].

Four square centimeter two-electrode supercapacitor cells have been assembled in acetonitrile + 1 M NEt_4BF_4 and galvanostatically cycled between 0 and 2.3 V. Fig. 4 presents the active material related capacitance change versus the current density, for two active material compositions: 95 wt.% AC–5 wt.% PTFE and 80 wt.% AC–15 wt.% MWCNTs–5 wt.% PTFE.

Results obtained without CNTs show that the activated carbon tested here allows a fast ionic migration inside the porosity. Whatever the active material composition, the behavior is roughly the same. The loss in capacitance is low, around 11% when the current density is increased from 5 up to 100 mA/cm^2. The increase of the power performances of the electrode, as noted before, does not limit the ionic migration kinetics inside the porous structure of the electrode at high current densities.

Table 1
Volumetric capacitance (calculated from Eq. (3)) obtained for the different active material compositions studied

Active material	C_v (F/cm^3)
95 wt.% AC, 5 wt.% PTFE	48 ($\pm$2.5)
80 wt.% AC, 15 wt.% CNTs, 5 wt.% PTFE	47 ($\pm$2.5)
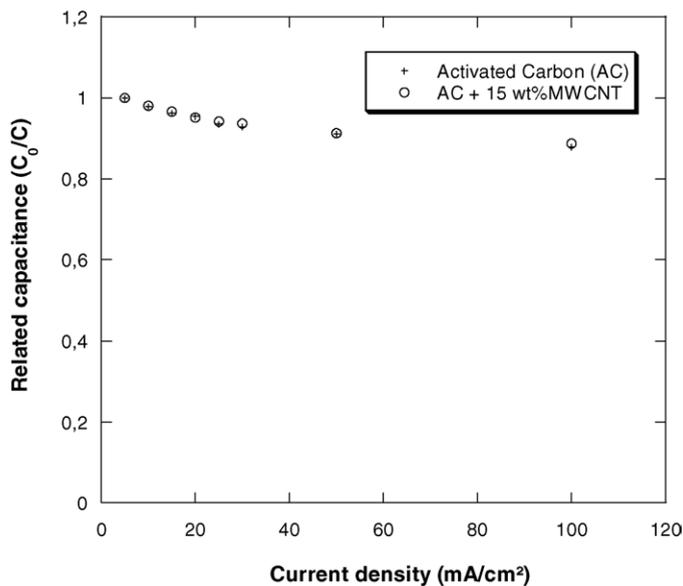
Fig. 4. Active material related capacitance (C/C_0) change vs. the supercapacitor cell current density.

A low-cost electronically conducting additive commonly used in batteries and supercapacitors active material is graphite and carbon black. Its electrochemical stability in most of the electrolytes used in electrochemical storage devices as well as its electronic conductivity make it suitable for such an utilization.

Results obtained with acetylene black (AB) and CNTs additions in the active material have been compared. Fig. 5 shows the ESR change during galvanostatic cycling between 0 and 2.3 V at ± 25 mA/cm^2 for the cells assembled with active material containing: 0 wt.% CNTs, 15 wt.% CNTs and 15 wt.% AB.

Cycling tests have been stopped at the 5000th cycles in order to limit the increase of water content inside the plexiglass sealed cell.

After stabilization (i.e. at the 100th cycle), the initial ESR values are, respectively, 0.7 and 0.6 Ω cm^2 for AB and CNTs-containing active material. These multiwall CNTs are then best candidates than AB to be used as conducting
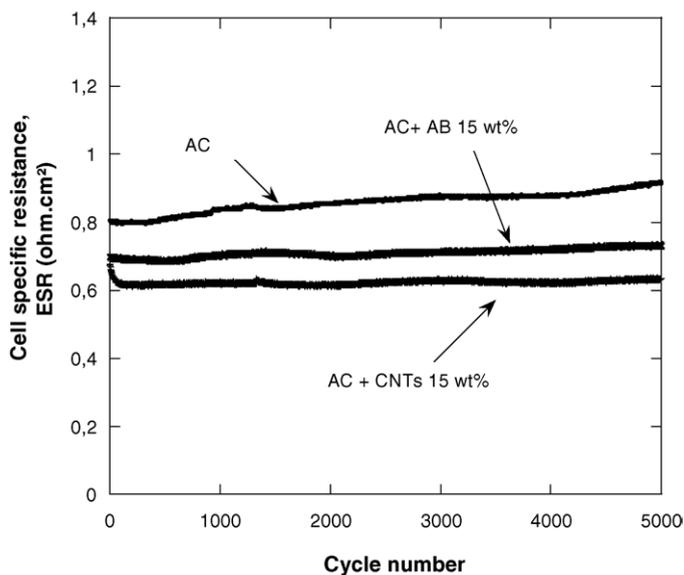
Fig. 5. ESR change during cycling between 0 and 2.3 V at ± 25 mA/cm^2 for the 4 cm^2 supercapacitor cells assembled with the different active material compositions. Active material weight: 60 mg per electrode; electrolyte NEt$_4$BF$_4$ 1.5 M in acetonitrile.

additives in the active materials in organic electrolytes. The results obtained mean that the ESR is decreased by 15% leading to an increase of specific power of 15%. During cycling, the specific capacitance for AB and CNTs-based active materials were found equal and constant at 87 F g^{-1}.

The stability of the ESR during cycling is not affected by the presence of AB or CNTs in the active material. On the contrary, it seems that the ESR stability is increased when 15 wt.% AB and then 15 wt.% CNTs are added to the activated carbon. This could be linked to the surface functions that are present onto the activated carbon surface and not (or few) on the AB and CNTs surface. These functional groups are well known to be responsible of self-discharge and instability during ageing under floating at high potential.

4. Conclusions

This paper presents the results obtained with supercapacitors using activated carbon/carbon nanotubes active material in non-aqueous electrolyte (NEt$_4$BF$_4$ 1 M in acetonitrile). The best results have been obtained with the active material containing 15 wt.% of CNTS laminated onto a treated-Al current collector. This composition in a two-electrode 4 cm^2 supercapacitor cell using 120 mg of active material gave promising results in terms of specific capacitance (88 F g^{-1}) and resistance (600 mΩ cm^2) and volumetric capacitance (47 F/cm^3). These values make these supercapacitors cells interesting for power applications.

Acknowledgement

References

[1] B.E. Conway, Electrochemical Supercapacitors, Kluwer Academic Publishers, Plenum Press, New York, 1999.
[2] P. Soudan, P. Lucas, H. Ang Ho, D. Jobin, L. Brean, D. Bélanger, J. Mater. Chem. 11 (2001) 773.
[3] A. Laforgue, P. Simon, J.F. Fauvarque, M. Mastragostino, F. Soavi, J.F. Sarrau, P. Lailler, M. Conte, E. Rossi, S. Saguatti, J. Electrochem. Soc. 150 (2003) A645.
[4] J.P. Zheng, P.J. Cygan, T.R. Jow, J. Electrochem. Soc. 142 (1995) 2699.
[5] T. Morimoto, K. Hiratsuka, Y. Sanada, K. Kurihara, J. Power Sources 60 (1996) 239.
[6] P.L. Taberna, P. Simon, J.F. Fauvarque, J. Electrochem. Soc. 150 (2003) A292.
[7] K. Koltz, M. Carlen, Electrochim. Acta 45 (2000) 2483–2498.
[8] A. Burke, J. Power Sources 91 (2000) 37.
[9] K. Jurewicz, K. Babel, A. Ziolkovsky, H. Wachovska, M. Kozlovski, Fuel Process. Technol. 77–78 (2002) 191.
[10] S. Yoon, J. Lee, T. Hyeon, S.M. Oh, J. Electrochem. Soc. 147 (7) (2000) 2507–2512.
[11] Ch. Emmenegger, P. Mauron, P. Sudan, V. Hermann, R. Galay, A. Züttel, J. Power Sources 124 (2003) 321–329.
[12] E. Frackowiak, K. Jurewicz, S. Delpeux, F. Beguin, J. Power Sources 97/98 (2001) 822.
[13] E. Frackowiak, F. Beguin, Carbon 39 (2001) 937.
[14] J.H. Chen, W.Z. Li, D.Z. Wang, S.X. Yang, J.G. Wen, Z.F. Ren, Carbon 40 (2002) 1193.
[15] B. Zhang, J. Liang, C.L. Xu, B.Q. Wei, D.B. Ruan, D.H. Wu, Mater. Lett. 51 (2001) 539–542.
[16] K.A. An, W.S. Kim, Y.S. Park, Y.C. Choi, S.M. Lee, D.C. Chung, D.J. Bae, S.C. Lim, Y.H. Lee, Adv. Mater. 13 (2001) 497.
[17] J.K.W. Sandler, J.E. Kirk, I.A. Kinloch, M.S.P. Schaffer, A.H. Windle, Polymer 44 (2003) 5893–5899.
[18] J. Gamby, P.L. Taberna, P. Simon, J.F. Fauvarque, M. Chesneau, J. Power Sources 101 (2001) 109.
[19] M. Endo, Y.J. Kim, H. Ohta, K. Ishii, T. Inoue, T. Hayashi, Y. Nishimura, T. Maeda, M.S. Dresselhaus, Carbon 40 (2002) 2613–2626.